

The Semiclassical Gluon Distribution at Next-to-Leading Order

H.G. Dosch, A. Hebecker, A. Metz and H.J. Pirner

*Institut für Theoretische Physik der Universität Heidelberg
Philosophenweg 16 & 19, D-69120 Heidelberg, Germany*

Abstract

The interaction of the partonic fluctuation of the virtual photon in deep inelastic scattering with soft color fields describing the hadron is treated in an eikonal approximation. It is known that, in this approach, the small- x limit of the leading-order gluon distribution $xg(x, Q^2)$ is a constant characterizing the averaged local field strength in the target. Matching the next-to-leading order calculation in this semiclassical framework with the one-loop parton model result, we obtain the next-to-leading order contribution to $xg(x, Q^2)$. It shows a $\ln(1/x)$ enhancement at small x and is sensitive to the large distance structure of the target. The final expression is a simple integral over non-Abelian eikonal factors measuring the target color field. We derive a quantitative relation between the short-distance cutoff of this integral and the scale of the gluon distribution function in the $\overline{\text{MS}}$ scheme. Our calculation demonstrates that higher order contributions can be systematically included in the semiclassical approach.

1 Introduction

The small- x limit of deep inelastic scattering (DIS) remains one of the most challenging problems on the interface of perturbative and non-perturbative QCD. It can be expected that both the perturbative physics described by QCD resummation techniques [1, 2] and the non-perturbative soft dynamics underlying the growth of total hadronic cross sections [3] are important for a complete picture of the small- x limit of structure functions. In this paper, we systematically relate models for the soft color fields, which we consider to be a promising tool for the characterization of the hadron, to the hadronic gluon distribution, which is the basic object of the perturbative treatment.

We are interested in a region of x and Q^2 where, although x is very small, the concept of parton distributions and the conventional DGLAP evolution equations [1] are applicable. For the description of the DIS process, the gluon distribution $g(x, \mu^2)$, which dominates in the small- x region, has to be given at some scale $\mu^2 < Q^2$. Thus, the problem of the non-perturbative structure of the target hadron has to be addressed.

Our basic starting point is the idea of describing high-energy processes in QCD by studying the eikonalized interaction of energetic partons with soft color fields [4, 5]. In this approach, which has been used for the description of DIS in [6], soft color fields in the center-of-mass frame of the collision mediate the interaction between the energetic projectile and target quarks. Progress towards the description of the energy dependence of cross sections in the framework of soft color field dynamics was reported, e.g., in [7].

A closely related approach to both inclusive and diffractive DIS, which treats the target proton as a superposition of soft color fields, was developed in [8, 9]. In fact, this semiclassical approach reproduces the treatment of [4–6] if the dynamics of the underlying color field is modelled on the basis of the stochastic vacuum [10] and a phenomenological ansatz for the constituent-quark wave function of the proton is made. For different approaches to the description of the target color fields see, e.g., [11]. However, in the following we are completely general and use no model-specific features of the target color field configurations or, equivalently, the wave functional of the proton.

In the present paper, the gluon distribution $g(x, \mu^2)$ at $x \ll 1$ and $\mu^2 \gg \Lambda^2$ (where Λ is a soft hadronic scale) is calculated for a target given by soft color field configurations. Here ‘soft’ means that all momentum components of the field are $\mathcal{O}(\Lambda)$. Following [12], a scalar ‘photon’, coupled directly to the gluon field, is used as a convenient theoretical tool for extracting the gluon distribution. The leading order calculation gives a constant for $x g(x, \mu^2)$, which is a measure for the averaged gluon field strength in the target. This is in agreement with the seminal paper of Mueller [12] and with [9], the spirit of which we follow closely.

In our opinion, it is crucial, both from a theoretical and a phenomenological perspective, to demonstrate the viability of the approach at higher orders. However, already at next-to-leading order the gluon distribution is scheme dependent and a careful matching of the partonic calculation (we use the $\overline{\text{MS}}$ scheme) and the semiclassical calculation is necessary to obtain an unambiguous result. With this result, we treat problems that were not addressed in the one-loop calculations of [12, 13], where the scheme dependence was

not discussed. In fact, the problems of regularization and scheme dependence arise immediately if one attempts to translate the one-loop, unintegrated gluon distribution of [13] into a correction to the leading term in the spirit of [9] (see [14] for a comparison of the results of [9] and [13] in the case of the quark distribution). As emphasized in [9], where diffractive and inclusive quark and gluon distributions were calculated in the semiclassical approach, the inclusive gluon distribution dominates the small- x region. Therefore, we expect that our next-to-leading order result is the dominant correction relevant as input for the next-to-leading order DGLAP evolution.

In our approach, the most intricate part is the semiclassical calculation at next-to-leading order. Working in Feynman gauge, we employ the optical theorem and calculate the forward scattering amplitude. In the high-energy limit, certain diagrams can be dropped. The remaining contribution is given in the form of a two-gluon production cross section. In this way, the identification with the parton model result becomes simple since the dangerous high-mass region, where the semiclassical approximation fails, cancels explicitly.

Let us note that, for a soft hadron governed by the single scale Λ , the perturbative expansion of the gluon distribution makes no sense. However, following ideas of [15] (see also the recent calculations of [16]), we can always assume that we are dealing with a very large target, in which case the gluon distribution becomes calculable without losing the interest of being genuinely non-perturbative in its origin (see [17] for a discussion of the new hard scale in a framework close to the present paper). It remains to be seen in how far this large-target approach will allow for a description of the qualitative features in the realistic proton case.

The paper is organized as follows. In Sect. 2 the scattering of a scalar photon off the target color field is calculated in the parton model and the semiclassical approach. The comparison of the two results gives rise to the leading-order semiclassical expression for the gluon distribution. In Sects. 3 and 4, the semiclassical and parton model calculations, respectively, are carried out at next-to-leading order. The extraction of the next-to-leading order contribution to the gluon distribution from the comparison of the semiclassical and the parton model results is the subject of Sect. 5. Section 6 contains our conclusions, and a number of technical details of the calculations are outlined in Appendices A–D.

2 The leading-order result

In the following analysis we use a scalar ‘photon’ coupled directly to the gluon field as a convenient theoretical tool for extracting the gluon distribution [12]. To be precise, the real ‘photon’ field χ couples to the field strength tensor $F_{\mu\nu}$ via the interaction Lagrangian

$$\mathcal{L}_I = -\frac{\lambda}{2} \chi \operatorname{tr} F_{\mu\nu} F^{\mu\nu}. \quad (1)$$

The leading-order amplitude for the scattering of the ‘photon’ off a classical color field is given by the diagram in Fig. 1.

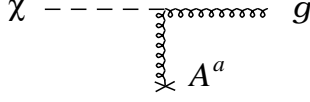


Figure 1: The process $\chi \rightarrow g$ in an external color field with one gluon exchange.

Let q and k be the momenta of the incoming virtual ‘photon’ ($q^2 = -Q^2$) and the outgoing gluon respectively. We define the light-cone components of a vector p by $p_{\pm} = p_0 \pm p_3$ and work in a frame where the plus components of q and k are large. In the high-energy limit, the amplitude \mathcal{T}^a corresponding to Fig. 1 is given in the rest frame of the proton by

$$i 2\pi \delta(k_0 - q_0) \mathcal{T}^a(\Delta_{\perp}) = -i\lambda \left(\frac{1}{2} k_+ \tilde{A}_-^a(\Delta) \right) (\epsilon_{\perp}^* \Delta_{\perp}). \quad (2)$$

Here $\Delta = k - q$, the field \tilde{A} is the Fourier transform of the external color field A , and ϵ is the polarization vector of the produced gluon. The evaluation of the r.h. side of Eq. (2) in the high-energy limit shows that \mathcal{T}^a does not depend on Δ_+ and Δ_- due to the softness of the external field. It is convenient to consider the impact parameter space amplitude

$$\tilde{\mathcal{T}}^a(x_{\perp}) = \frac{i\lambda q_0}{2C_A} \int dx_+ \text{tr} [T^a(\epsilon_{\perp}^* \partial_{\perp}) A_-^A(x_+, x_{\perp})] \quad (3)$$

(with $\partial_{\perp} \equiv \partial/\partial x_{\perp}$), which is related to the amplitude in Eq. (2) by a Fourier transformation in transverse space. The x_- dependence of A^A is irrelevant in the high-energy limit. Here $A^A = A^b T^b$ and T^b are the generators of $SU(N_c)$ in the adjoint representation, which we use throughout this paper; $C_A = N_c$.

Resumming the gluon exchange to all orders means that the fast gluon created at the initial χgg vertex acquires a non-Abelian eikonal factor while travelling through the rest of the external field. This is illustrated in Fig. 2.

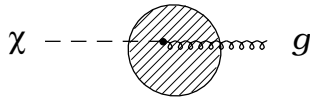


Figure 2: The process $\chi \rightarrow g$ in an external color field. The dot symbolizes the initial χgg vertex.

The transition to the resummed amplitude of Fig. 2 is realized by the substitution

$$\partial_{\perp} A_-^A \longrightarrow U_{(\infty, x_+)}^A(x_{\perp}) \partial_{\perp} A_-^A U_{(\infty, x_+)}^{A\dagger}(x_{\perp}) \quad (4)$$

in Eq. (3), where

$$U_{(\infty, x_+)}^A(x_{\perp}) = P \exp \left[-\frac{ig}{2} \int_{x_+}^{\infty} dx_+ A_-^A(x_+, x_{\perp}) \right]. \quad (5)$$

The operator P denotes path ordering along x_+ .

From this, the total cross section for the scattering of the virtual photon off the color field target, i.e., the semiclassical (*sc*) leading-order result, can be derived. Using the identity

$$\int_{-\infty}^{\infty} dx_+ U_{(\infty, x_+)}^{\mathcal{A}}(x_{\perp}) (\partial_{\perp} A_{-}^{\mathcal{A}}(x_+, x_{\perp})) U_{(x_+, -\infty)}^{\mathcal{A}}(x_{\perp}) = \left(-\frac{2}{ig}\right) \partial_{\perp} U_{(\infty, -\infty)}^{\mathcal{A}}(x_{\perp}), \quad (6)$$

one finds

$$\sigma_{sc}^{(0)}(x, Q^2) = \frac{\lambda^2}{4g^2 C_A} \int d^2 x_{\perp} \left| \frac{\partial}{\partial y_{\perp}} W_{x_{\perp}}^{\mathcal{A}}(y_{\perp}) \Big|_{y_{\perp}=0} \right|^2 \equiv \frac{\lambda^2}{4g^2 C_A} \int d^2 x_{\perp} |\partial_{\perp} W_{x_{\perp}}^{\mathcal{A}}(0_{\perp})|^2, \quad (7)$$

where the index (0) stands for ‘leading order’. Here

$$W_{x_{\perp}}^{\mathcal{A}}(y_{\perp}) = U^{\mathcal{A}}(x_{\perp}) U^{\mathcal{A}\dagger}(x_{\perp} + y_{\perp}) - 1 \quad (8)$$

and

$$U^{\mathcal{A}}(x_{\perp}) = U_{(\infty, -\infty)}^{\mathcal{A}}(x_{\perp}). \quad (9)$$

In Eq. (7), the summation over color indices is implicit. In the following it is always assumed that an appropriate averaging over the color fields underlying the basic quantity $W^{\mathcal{A}}$ is performed (cf. [9]).

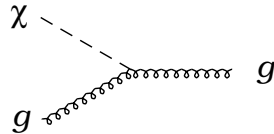


Figure 3: The partonic process $\chi g \rightarrow g$ at leading order.

The leading-order semiclassical gluon distribution is obtained by comparing this result with a conventional partonic calculation, where the target is described by a gluon distribution. The relevant diagram is shown in Fig. 3, and the corresponding parton model (*pm*) cross section reads

$$\sigma_{pm}^{(0)}(x, Q^2) = \frac{\pi \lambda^2}{4} x g^{(0)}(x, Q^2). \quad (10)$$

Identifying the cross sections of Eqs. (7) and (10), one obtains

$$x g^{(0)}(x, Q^2) = \frac{1}{2\pi^2 \alpha_s} \frac{1}{2C_A} \int d^2 x_{\perp} |\partial_{\perp} W_{x_{\perp}}^{\mathcal{A}}(0_{\perp})|^2. \quad (11)$$

This result has been derived in [9] identifying the scaling violations of F_2 with the gluon distribution. Note the color factor $\frac{1}{2C_A}$ in Eq. (11) due to the adjoint representation, which we use throughout the paper. As expected, this leading-order gluon distribution $x g^{(0)}(x, Q^2)$ is constant for $x \rightarrow 0$ and shows no scaling violations beyond those induced by the explicit α_s -factor on the r.h. side of Eq. (11). In [6] the value of $\lim_{x \rightarrow 0} x g(x, Q^2)$ has been given in the stochastic vacuum model.

3 Semiclassical calculation at next-to-leading order

The leading $\ln Q^2$ calculation of the process $\chi \rightarrow gg$ in the semiclassical approach reproduces the conventional gluon-gluon splitting function, as shown in [9]. Here, we need the complete next-to-leading order total cross section for the scattering of a χ particle off an external color field. This calculation can be simplified significantly if one starts with a discussion of all diagrams contributing to the forward amplitude. The total cross section follows from the imaginary part of this amplitude. Furthermore, it is convenient to begin by considering the two-gluon exchange approximation.

Clearly, the leading order diagram for the forward amplitude is simply the square of Fig. 1. At next-to-leading order, all the diagrams in Fig. 4 have to be considered.

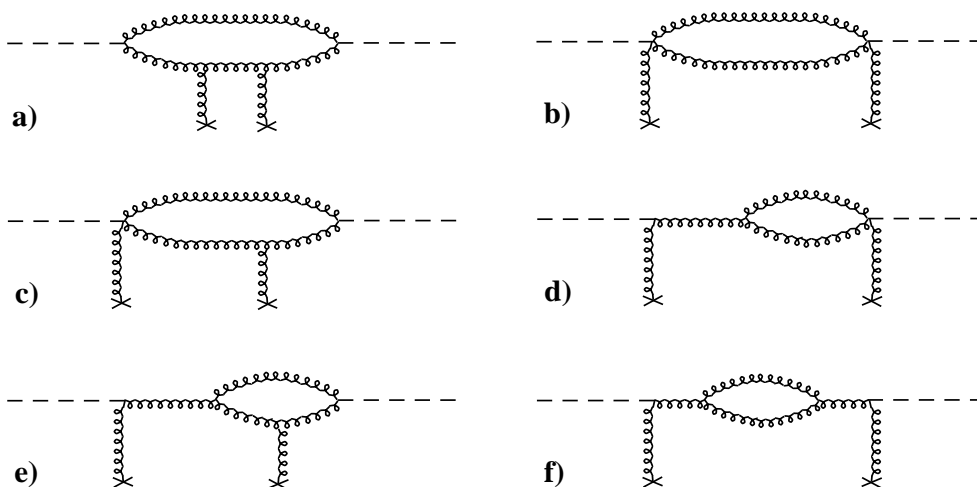


Figure 4: Two-gluon exchange diagrams for the forward scattering of the scalar ‘photon’ χ off a color field. The mirrored analogues of c), d) and e) and the analogue of graph a) with the two t channel gluons attached to different horizontal lines are not shown.

In the high-energy limit, the diagrams d), e) (with their mirrored analogues) and diagram f) do not contribute. This can be understood intuitively by recalling that the gluon field is localized in a given region of space. Therefore, in the limit of infinite plus momentum, the right-moving gluonic degrees of freedom have no time for a virtual fluctuation between their first and second interaction with the external field (see Appendix A for a more technical argument). A related discussion in the case of particle radiation in high-energy scattering of external fields can be found in [18].

What remains to be calculated is the imaginary part of diagram a) (and the corresponding diagram where the two t channel gluons are attached to different lines), diagram b) and diagram c) (with its mirrored analogue). This corresponds to calculating the cross section for $\chi \rightarrow gg$ from the amplitude defined by the three diagrams in Fig. 5. Note that this is a significant simplification since the amplitude in Fig. 5 has no contributions arising from cutting diagrams d), e) and f) of Fig. 4.

The next step is to resum the interaction with the external field to all orders, i.e., to repeat the step leading from Fig. 1 to Fig. 2. The result is illustrated in Fig. 6. Here, the

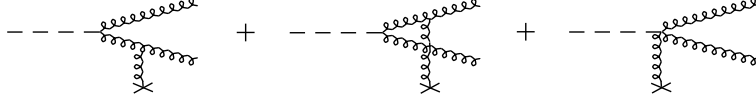


Figure 5: The simplified amplitude for $\chi \rightarrow gg$, which can be used for the calculation of the total cross section.

first diagram corresponds to the fluctuation of the incoming ‘photon’ into a gg pair before the target and the subsequent scattering of the gluons off the color field, treated in the eikonal approximation. In an expansion in powers of the external field, the leading term reproduces the first two diagrams of Fig. 5. The second diagram of Fig. 6 corresponds to the creation of the two gluons in the space-time region of the external field, via a χggg vertex. The two fast gluons then acquire non-Abelian eikonal phases while travelling through the rest of the color field. An expansion in powers of the external field generates the third diagram of Fig. 5.

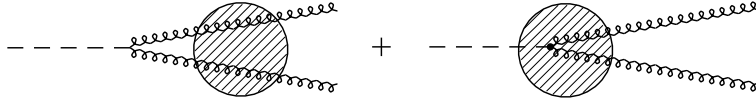


Figure 6: The relevant contributions to the amplitude in the next-to-leading order semiclassical calculation. The dot in the second diagram symbolizes the initial χggg vertex.

The amplitude of Fig. 6 can be calculated using the methods of [8] (see also [19]). Some details relevant to this particular process are discussed in Appendix B. The result can be given in the form

$$\sigma_{sc}^{(1)}(x, Q^2) = \frac{\lambda^2}{32(2\pi)^6} \int d\alpha \int \frac{dk_{\perp}^2}{\alpha(1-\alpha)} \int d^2x_{\perp} \left| \int d^2k_{\perp} \frac{N^2 \delta_{ij} + 2k_i k_j}{N^2 + k_{\perp}^2} \tilde{W}_{x_{\perp}}^{\mathcal{A}}(k'_{\perp} - k_{\perp}) \right|^2, \quad (12)$$

where α and $1 - \alpha$ are the longitudinal momentum fractions carried by the two gluons, $N^2 = \alpha(1 - \alpha)Q^2$, k_{\perp} and k'_{\perp} are the transverse momenta of one of the two gluons before and after the interaction with the external field respectively, and $\tilde{W}^{\mathcal{A}}$ is the Fourier transform of the function defined in Eq. (8). Summation over the indices i, j and over the color indices of $\tilde{W}^{\mathcal{A}}$ is implicit.

The full next-to-leading order semiclassical result is given by the sum of Eqs. (7) and (12):

$$\sigma_{sc}(x, Q^2) = \sigma_{sc}^{(0)}(x, Q^2) + \sigma_{sc}^{(1)}(x, Q^2). \quad (13)$$

4 Parton model result at next-to-leading order

Working in $d = 4 + \epsilon$ dimensions, the amplitude corresponding to Fig. 7, which includes a factor $1/(2 + \epsilon)$ for initial state gluon polarization, a factor $1/2$ for identical final state

particles, and the color factor $C_A = N_c$, reads

$$|\mathcal{T}_{\chi g \rightarrow gg}|^2 = \frac{C_A}{2} \lambda_d^2 g_d^2 \left\{ \frac{1}{2\hat{s}\hat{t}\hat{u}} (\hat{s}^4 + \hat{t}^4 + \hat{u}^4 + Q^8) - \frac{2\epsilon}{2+\epsilon} Q^2 \right\}. \quad (14)$$

Here $\lambda_d = \lambda\mu^{-\epsilon/2}$ and $g_d = g\mu^{-\epsilon/2}$ are the d -dimensional couplings, and $\hat{s}, \hat{t}, \hat{u}$ are the usual Mandelstam variables of a 2-to-2 scattering process.

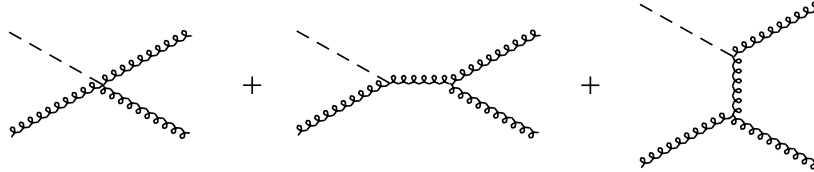


Figure 7: Conventional partonic amplitude for the process $\chi g \rightarrow gg$. The crossed contribution belonging to the last of the three graphs and the ghost diagrams that have to be added for covariant polarization summation are not shown.

From this squared amplitude, the total partonic cross section $\hat{\sigma}^{(1)}(z, Q^2)$ for the process $\chi g \rightarrow gg$ is obtained by standard methods. The variable z is defined by $z = Q^2/(Q^2 + \hat{s})$. Alternatively, it is given by $z = x/y$, where y is the fraction of the target momentum carried by the struck gluon. Combining this with the leading order result, one can write

$$\sigma_{pm}(x, Q^2) = \int_x^1 \frac{dz}{z} \left(\sigma_{0\{d\}} \delta(1-z) + \hat{\sigma}^{(1)}(z, Q^2) \right) yg_b(y), \quad (15)$$

where $\sigma_{0\{d\}} = \pi\lambda_d^2/4$ (cf. Eq. (10)). Note that in the following we only calculate terms enhanced by powers of $\ln(1/x)$. Therefore virtual corrections, which affect only the endpoint $z = 1$ and do not produce such terms, do not contribute.

Working in the $\overline{\text{MS}}$ scheme, we renormalize the bare gluon distribution $g_b(x)$ according to

$$g_b(x) = g(x, \mu^2) - \frac{\alpha_s}{2\pi} \int_x^1 \frac{dz}{z} P_{gg}(z) \left\{ \frac{2}{\epsilon} + \gamma_E - \ln 4\pi \right\} g(y, \mu^2). \quad (16)$$

The result can finally be given in the form

$$\sigma_{pm}(x, Q^2) = \sigma_{0\{d=4\}} x \int_x^1 \frac{dz}{z} \left(\delta(1-z) + \frac{\alpha_s}{2\pi} \left[P_{gg}(z) \ln \frac{Q^2}{\mu^2} + C_g^{\overline{\text{MS}}}(z) \right] \right) g(y, \mu^2), \quad (17)$$

where the integrand is only complete in the region $z < 1$. In Eq. (17) $P_{gg}(z)$ (with $z < 1$) is the usual gluon-gluon splitting function. The coefficient function $C_g^{\overline{\text{MS}}}(z)$, characteristic of the process under consideration, has been derived to be

$$C_g^{\overline{\text{MS}}}(z) = P_{gg}(z) \ln \frac{1-z}{z} - \frac{11C_A}{6z(1-z)}. \quad (18)$$

5 Extracting the gluon distribution

As in the leading-order case discussed in Sect. 2, the gluon distribution is extracted from the next-to-leading order semiclassical calculation by identifying the next-to-leading order total cross sections of the semiclassical and the parton model approach given by Eqs. (13) and (17): $\sigma_{sc}(x, Q^2) = \sigma_{pm}(x, Q^2)$.

We write the gluon distribution $xg(x, \mu^2)$ entering Eq. (17) as

$$xg(x, \mu^2) = xg^{(0)}(x, \mu^2) + xg^{(1)}(x, \mu^2), \quad (19)$$

where $xg^{(0)}(x, \mu^2)$ is given by Eq. (11) and $xg^{(1)}(x, \mu^2)$ is a higher-order correction. Inserting Eq. (19) into Eq. (17), both $g^{(0)}$ and $g^{(1)}$ are kept in the $\delta(1-z)$ term, but only the leading-order distribution $g^{(0)}$ is kept in the α_s contribution. Now, identifying σ_{sc} and σ_{pm} , the leading order parts of both cross sections cancel and one finds

$$\begin{aligned} xg^{(1)}(x, \mu^2) &= \frac{1}{4(2\pi)^7} \int d\alpha \int \frac{dk_{\perp}^{\prime 2}}{\alpha(1-\alpha)} \int d^2x_{\perp} \left| \int d^2k_{\perp} \frac{N^2 \delta_{ij} + 2k_i k_j}{N^2 + k_{\perp}^2} \tilde{W}_{x_{\perp}}^{\mathcal{A}}(k'_{\perp} - k_{\perp}) \right|^2 \\ &\quad - \frac{\alpha_s}{2\pi} \int_x^1 dz \left[P_{gg}(z) \ln \frac{Q^2}{\mu^2} + C_g^{\overline{\text{MS}}}(z) \right] yg^{(0)}(y, \mu^2). \end{aligned} \quad (20)$$

When evaluating the r.h. side of this equation, all terms that are not enhanced by $\ln(1/x)$ will be dropped. In particular, we can use

$$P_{gg}(z) \simeq \frac{2C_A}{z} \quad \text{and} \quad C_g^{\overline{\text{MS}}}(z) \simeq \frac{2C_A}{z} \left(\ln \frac{1}{z} - \frac{11}{12} \right). \quad (21)$$

Note that in Eq. (20) we are only interested in the leading twist contribution of the semiclassical cross section which will be determined in Eq. (22).

The integral involving the function $\tilde{W}^{\mathcal{A}}$ is conveniently rewritten using the integration variable $z = Q^2/(Q^2 + M^2)$, where $M^2 = \hat{s} = k_{\perp}^{\prime 2}/(\alpha(1-\alpha))$ is the invariant mass of the two gluons in the final state. We introduce a parameter μ' such that, for a soft hadronic scale Λ governing the behaviour of $\tilde{W}^{\mathcal{A}}$, one has $\Lambda^2 \ll \mu'^2 \lesssim Q^2$. This allows us to decompose the integral according to (see Appendix C for details)

$$\begin{aligned} &\frac{1}{4(2\pi)^7} \int d\alpha \int \frac{dk_{\perp}^{\prime 2}}{\alpha(1-\alpha)} \int d^2x_{\perp} \left| \int d^2k_{\perp} \frac{N^2 \delta_{ij} + 2k_i k_j}{N^2 + k_{\perp}^2} \tilde{W}_{x_{\perp}}^{\mathcal{A}}(k'_{\perp} - k_{\perp}) \right|^2 \\ &= \frac{1}{4\pi^3} \int^1 \frac{dz}{z} \ln \frac{Q^2}{z\mu'^2} \int d^2x_{\perp} |\partial_{\perp} W_{x_{\perp}}^{\mathcal{A}}(0_{\perp})|^2 + \frac{2}{\pi} \int^1 \frac{dz}{z} \int_0^{\mu'^2} dk_{\perp}^{\prime 2} f(k_{\perp}^{\prime 2}), \end{aligned} \quad (22)$$

where the non-perturbative $W^{\mathcal{A}}$ dependence is encoded in the function f :

$$f(k_{\perp}^{\prime 2}) = \int \frac{d^2y_{\perp}}{(2\pi)^2 y_{\perp}^2} \int \frac{d^2z_{\perp}}{(2\pi)^2 z_{\perp}^2} \int d^2x_{\perp} \text{tr} [W_{x_{\perp}}^{\mathcal{A}}(y_{\perp}) W_{x_{\perp}}^{\mathcal{A}\dagger}(z_{\perp})] e^{ik'_{\perp}(y_{\perp} - z_{\perp})} \left(\frac{2(y_{\perp} z_{\perp})^2}{y_{\perp}^2 z_{\perp}^2} - 1 \right). \quad (23)$$

Here and in the following we disregard all terms suppressed by powers of Λ^2/μ'^2 . The motivation for writing the integral in the form given in Eq. (22) is the explicit separation of the $\ln Q^2$ term, which is multiplied by the short-distance specific function $\partial_\perp W_{x_\perp}^A(0_\perp)$.

Note that we have not specified the lower bound of the z integrations in Eq. (22). Clearly, the kinematical limit is $z = x$ since the invariant mass of the produced gg pair can not be larger than the total center-of-mass energy available. However, no such bound appears explicitly in the semiclassical treatment since the classical color field behaves like an infinitely heavy target. The physical cutoff is provided by the breakdown of the semiclassical approximation for $z \sim x$, i.e., $y \sim 1$.

Therefore, in order to obtain the leading logarithm, the second term on the r.h. side of Eq. (22) has to be treated by applying the substitution

$$\int^1 \frac{dz}{z} \longrightarrow \ln \frac{1}{x}. \quad (24)$$

For the first term on the r.h. side of Eq. (22), only the short distance structure of the external field matters. According to Eq. (11), this short distance behaviour is characterized by the leading order gluon distribution $yg^{(0)}(y, \mu^2)$. Thus, we substitute

$$\frac{1}{2C_A} \int^1 \frac{dz}{z} \ln \frac{Q^2}{z\mu'^2} \int d^2x_\perp |\partial_\perp W_{x_\perp}^A(0_\perp)|^2 \longrightarrow \int_x^1 \frac{dz}{z} \ln \frac{Q^2}{z\mu'^2} 2\pi^2 \alpha_s(\mu^2) yg^{(0)}(y, \mu^2) \quad (25)$$

and assume that the behaviour of the phenomenological gluon distribution at $z \rightarrow x$, i.e., $y = x/z \rightarrow 1$, correctly accounts for the region where the semiclassical treatment is no longer valid. In fact, when inserting Eq. (22) with the substitutions Eq. (24) and (25) into Eq. (20), the details of the large- y behaviour of $yg^{(0)}(y, \mu^2)$ do not matter since the $\ln^2(1/x)$ enhanced contributions from the semiclassical and the partonic calculations cancel. Thus, we obtain

$$xg^{(1)}(x, \mu^2) = \ln \frac{1}{x} \left[\frac{\alpha_s}{\pi} C_A \left(\ln \frac{\mu^2}{\mu'^2} + \frac{11}{12} \right) xg^{(0)}(x, \mu^2) + \frac{2}{\pi} \int_0^{\mu'^2} dk'_\perp{}^2 f(k'_\perp{}^2) \right], \quad (26)$$

where the μ'^2 dependence cancels between the two terms. Therefore, we can set $\mu'^2 = \mu^2 \exp[11/12]$ and write

$$xg^{(1)}(x, \mu^2) = \frac{2}{\pi} \left(\ln \frac{1}{x} \right) \int_0^{\mu^2 \exp[11/12]} dk'_\perp{}^2 f(k'_\perp{}^2). \quad (27)$$

Note that the correction $xg^{(1)}(x, \mu^2)$ shows scaling violations consistent with the Altarelli-Parisi evolution at small x and a logarithmic small- x enhancement that is sensitive to the non-perturbative, large-size structure of the target.

It would be interesting to evaluate Eq. (27) in the framework of the model of the stochastic vacuum of [5] or of the large hadron model employed in [9]. Note in particular that, following [9], the large- N_c expression

$$\int d^2x_\perp \text{tr} \left(W_{x_\perp}^A(y_\perp) W_{x_\perp}^{A\dagger}(z_\perp) \right) = \Omega N_c^2 \left[1 - e^{-ay_\perp^2} - e^{-az_\perp^2} + e^{-a(y_\perp - z_\perp)^2} \right] \quad (28)$$

can be used in Eq. (23). Here Ω is the geometrical cross section of the target, the impact parameter dependence of the target thickness (which would be reflected in an impact parameter dependence of the parameter a) is neglected, and averaging over all relevant color field configurations is assumed. With this model, the unintegrated, i.e., k'_\perp dependent, version of $xg^{(1)}(x, \mu^2)$ reproduces the recent result of Mueller (cf. Eq. (44) of [13]). The result presented in Eq. (27) extends the discussion given in [13] by carefully matching the semiclassical and the parton model calculations. This gives rise to a precise definition of the cutoff of the k'_\perp integration in Eq. (27) and to the interpretation of the result as a correction to the leading order gluon distribution of Eq. (11).

Equations (23) and (27) can be significantly simplified (cf. Appendix D for details) leading to the main result of our paper:

$$xg^{(1)}(x, \mu^2) = \frac{1}{\pi^3} \left(\ln \frac{1}{x} \right) \int_{r(\mu)^2}^{\infty} \frac{dy_\perp^2}{y_\perp^4} \left\{ - \int d^2x_\perp \text{tr} W_{x_\perp}^A(y_\perp) \right\}, \quad r(\mu)^2 = \frac{4e^{\frac{1}{12} - 2\gamma_E}}{\mu^2}. \quad (29)$$

It is easy to see how such a formula comes about: if the cutoff μ^2 in Eq. (27) could be taken to infinity, the integration $dk'_\perp{}^2 = d^2k'_\perp/\pi$ would give rise to the δ -function $\delta^2(y_\perp - z_\perp)$ (cf. Eq. (23)), and either the y_\perp or the z_\perp integration could be trivially performed. The remaining integration, say the y_\perp integration, is now divergent at small y_\perp , showing that the cutoff in Eq. (27) can, in fact, not be removed. The integrand of this divergent y_\perp integration is precisely the one of Eq. (29) and, as can be seen by closer inspection of the relevant integrals (cf. Appendix D), it is possible to translate the upper cutoff of the k'_\perp integration into a lower cutoff of the y_\perp integration. This is the origin of the compact formula in Eq. (29).

Given a specific model for the gluon fields of the target that allows for the calculation of the fundamental quantity $W_{x_\perp}^A(y_\perp)$, Eq. (29) can be used to improve the leading order semiclassical result of Eq. (11).

With the large- N_c expression of [9],

$$-2 \int d^2x_\perp \text{tr} W_{x_\perp}^A(y_\perp) = \int d^2x_\perp \text{tr} \left(W_{x_\perp}^A(y_\perp) W_{x_\perp}^{A\dagger}(y_\perp) \right) = 2\Omega N_c^2 \left[1 - e^{-ay_\perp^2} \right], \quad (30)$$

one can see the qualitative agreement of Eq. (29) with Eqs. (49)–(51) of [12]. The progress of the present investigation is the careful matching of the semiclassical and the parton model treatment, giving rise to the precise definition of the cutoff of the y_\perp integration in terms of the scale of the gluon distribution.

6 Summary and conclusions

The semiclassical approach has been successfully applied to different kinds of high-energy reactions. In DIS, the interaction of the energetic partons of the photon with the target can be calculated in the eikonal approximation and is essentially given by a (non-perturbative) Wegner-Wilson loop, which measures an integral of the field strength of the target.

This approach, though limited to low scales μ^2 , can predict input distributions for the DGLAP equation. Of course, in order to make numerical estimates of the parton densities, the evaluation of the Wegner-Wilson loop in a specific non-perturbative model is necessary.

In this respect the gluon distribution is of particular interest as it dominates DIS at low x . To leading order, the distribution $x g^{(0)}(x, \mu^2)$ is a constant characterizing the averaged local field strength in the target. Therefore, a calculation at next-to-leading order is mandatory to obtain a nontrivial energy dependence of the gluon density.

Using a scalar ‘photon’ (denoted by χ), which couples directly to the gluon in a gauge invariant way, we derive the gluon density by matching the semiclassical and the parton model approach. At leading order, we have to equate the cross section for the transition $\chi \rightarrow g$ in a soft external field with the cross section of the process $\chi g \rightarrow g$ as given in the parton model. At next-to-leading order, the cross section for the transition $\chi \rightarrow gg$ in a soft external field has to be equated with the parton model cross section of the process $\chi g \rightarrow gg$. The α_s correction of the gluon distribution shows a logarithmic enhancement, i.e., $x g^{(1)}(x, \mu^2) \propto \ln(1/x)$.

In our approach we can not go beyond the leading- $\ln(1/x)$ approximation. This is a fundamental limitation of the semiclassical treatment and many related approaches, which has its origin in the artificial separation of the QCD dynamics into the soft degrees of freedom of the target and the high-energy modes of the projectile. Integrating over the fluctuations of the projectile, one has to drop the soft modes since their interaction can not be treated in the eikonal approximation.

Parton distributions at next-to-leading order are scheme dependent. Our final result in Eq. (29) (together with the leading order contribution of Eq. (11)) provides the gluon density in the $\overline{\text{MS}}$ scheme. The short-distance cutoff in Eq. (29) is quantitatively related to the scale of the gluon distribution. This enables us to obtain numerical predictions for the gluon distribution at next-to-leading order in any non-perturbative approach describing the soft color field of the proton.

Acknowledgements

One of us (A.H.) would like to thank W. Buchmüller and T. Gehrmann for the fruitful collaboration on a previous paper, during which essential ideas underlying this present investigation took shape.

A Suppression of intermediate virtual fluctuations in the high-energy limit

To illustrate the vanishing of diagrams d), e) and f) of Fig. 4 in the high-energy limit, consider first the simpler case where the horizontal gluon lines are replaced by scalar lines. The scalar version of diagram Fig. 4d) with the naming of momenta used in this appendix is shown in Fig. 8.

In the high-energy limit, the soft external field can not change the momentum plus

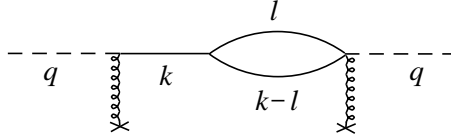


Figure 8: Scalar version of diagram Fig. 4d).

component of the fast right-moving particles essentially, $k_+ \simeq q_+$. Furthermore, the dependence of the external field vertex on the minus component of the transferred momentum can be neglected. Thus, the minus component integrations in the diagram Fig. 8 take the form

$$I = \int dk_- \int dl_- \frac{1}{[k_+ k_- - k_\perp^2 + i\epsilon] [l_+ l_- - l_\perp^2 + i\epsilon] [(k-l)_+ (k-l)_- - (k-l)_\perp^2 + i\epsilon]}. \quad (31)$$

Note first that this expression vanishes unless $0 \leq l_+ \leq k_+$, in which case the two poles in the complex l_- plane lie on different sides of the integration contour. However, this means that both k_+ and $(k-l)_+$ have to be positive, so that now both poles in the complex k_- plane are on the same side of the integration contour. This demonstrates that the integral I vanishes in any case.

The same argument applies to the scalar analogues of diagrams Fig. 4e) and f), since there the momentum k also flows through more than one propagator between the two external field vertices. This results in the presence of several poles in k_- , all on the same side of the integration contour, and therefore in the vanishing of the integral.

All that has been said above applies to the gluonic case as well, as long as there is no additional minus component dependence introduced by the numerator factors. Such a dependence would prevent us from closing the integration contour. Working in Feynman gauge and applying the decomposition of the gluon propagator given in Appendix B to the lines with momentum k , one can easily convince oneself that, in the high-energy limit, there is indeed no dependence on the minus components.

Thus, we are justified in disregarding diagrams Fig. 4d) – f) when calculating the forward scattering amplitude at next-to-leading order.

B Details of the next-to-leading order semiclassical calculation

The l.h. diagram of Fig. 6 contains three contributions: two of them describe the interaction of a single outgoing gluon with the color field, whereas in the third case both gluons interact with the field. Here we consider the latter case as an example, and outline some crucial steps of the evaluation of the corresponding amplitude which we call \mathcal{T}^{gg} .

Working in Feynman gauge and denoting the momenta of the gluons before (after)

the interaction by k and p (k' and p'), respectively, the amplitude reads

$$i2\pi\delta(k'_0 + p'_0 - q_0)\mathcal{T}_{ij}^{gg} = \int \frac{d^4k}{(2\pi)^4} \epsilon_{(i)}^{\alpha*}(p') V_{\alpha\mu}(p', p) \frac{-ig^{\mu\rho}}{p^2} H_{\rho\sigma}(p, k) \frac{-ig^{\sigma\nu}}{k^2} V_{\nu\beta}^\dagger(k', k) \epsilon_{(j)}^{\beta*}(k'), \quad (32)$$

where the indices i, j characterize the polarization of the gluons in the final state. The quantity H represents the χgg vertex,

$$H_{\rho\sigma}(p, k) = i\lambda((kp)g_{\rho\sigma} - k_\rho p_\sigma), \quad (33)$$

while $V(p', p)$ and $V(k', k)$, which will be explicitly given below, are the effective vertices for the scattering of the fast gluons off the external field.

To simplify the calculation we exploit an alternative representation of the metric tensor appearing in the gluon propagators. For instance, the tensor $g^{\mu\rho}$ of the propagator $-ig^{\mu\rho}/p^2$ is decomposed according to

$$g^{\mu\rho} = -\sum_{i=1}^2 \epsilon_{(i)}^\mu(p) \epsilon_{(j)}^\rho(p) + \frac{n^\mu p^\rho}{np} + \frac{p^\mu n^\rho}{np} - \frac{n^\mu n^\rho}{(np)^2} p^2, \quad (34)$$

with the light like vector $n = (n_+, n_-, n_\perp) = (0, 2, 0_\perp)$. A possible choice of the polarization vectors $\epsilon_{(i)}(p)$ in Eq. (34), which in particular satisfy $\epsilon_{(i)}(p)p = 0$, is given by

$$\epsilon_{(i)}(p) = \left(0, \frac{2p_\perp \epsilon_{(i)\perp}}{p_+}, \epsilon_{(i)\perp}\right), \quad (35)$$

with the transverse basis $\epsilon_{(1)\perp} = (1, 0)$ and $\epsilon_{(2)\perp} = (0, 1)$.

In the high energy limit, the t channel exchange of gluons leads to an amplitude which is proportional to q_+ . As a consequence, in order to obtain the leading part of the amplitude, in Eq. (34) only the term containing the polarization vectors has to be considered. Because of gauge invariance of the χgg vertex the second term on the r.h. side of Eq. (34) vanishes. The contribution of the remaining two terms is at most proportional to $(q_+)^0$ and hence negligible.

The effective vertices are now multiplied by the polarization vectors of two on-shell gluons; these vertices are governed by the non-Abelian eikonal factor defined in Eqs. (9) and (5). One finds

$$\epsilon_{(i)}^\alpha(p') V_{\alpha\mu}(p', p) \epsilon_{(j)}^\mu(p) = 2\pi\delta(p'_0 - p_0) 2p_0 \left[\tilde{U}^{\mathcal{A}}(p'_\perp - p_\perp) - (2\pi)^2 \delta^2(p'_\perp - p_\perp) \right] \delta_{ij}, \quad (36)$$

and an analogous expression for the second vertex. The contribution proportional to $\delta^2(p'_\perp - p_\perp)$ subtracts the term in $\tilde{U}^{\mathcal{A}}$ which contains no interaction, while δ_{ij} indicates conservation of the gluon helicity. In Ref. [19] the interested reader can find more details of the derivation of Eq. (36).

Writing the loop integration in terms of light cone variables, $d^4k = (1/2)dk_+ dk_- d^2k_\perp$, and using the approximation $\delta(k'_0 - k_0) \simeq 2\delta(k'_+ - k_+)$ we arrive at

$$\begin{aligned} \mathcal{T}_{ij}^{gg} &= -\frac{\lambda}{2(2\pi)^3} q_+^2 \int dk_- d^2k_\perp \frac{1}{k^2 p^2} \left[\alpha(1-\alpha)(Q^2 + k^2 + p^2) \delta_{ij} + 2k_i k_j \right] \\ &\quad \times \left[\tilde{U}^{\mathcal{A}}(p'_\perp - p_\perp) - (2\pi)^2 \delta^2(p'_\perp - p_\perp) \right] \left[\tilde{U}^{\mathcal{A}\dagger}(k'_\perp - k_\perp) - (2\pi)^2 \delta^2(k'_\perp - k_\perp) \right]. \end{aligned} \quad (37)$$

The diagram on the r.h. side of Fig. 6 cancels the k^2 and p^2 term in the expression $(Q^2 + k^2 + p^2)$ of Eq. (37). Now, the k_- integration can be performed by closing the integration contour in the lower half of the complex k_- plane.

The resulting expression contains terms proportional to $\tilde{U}^A \tilde{U}^{A\dagger}$, \tilde{U}^A , and $\tilde{U}^{A\dagger}$, as well as a constant term. The two additional contributions, where only a single gluon interacts with the external field and which belong to the l.h. side of Fig. 6, contain terms proportional to \tilde{U}^A and $\tilde{U}^{A\dagger}$ and a constant term. If one adds these contributions, the color field dependence of the total amplitude \mathcal{T}_{ij} turns out to be

$$\begin{aligned} & \tilde{U}^A(p'_\perp - p_\perp) \tilde{U}^{A\dagger}(k'_\perp - k_\perp) - (2\pi)^4 \delta^2(p'_\perp - p_\perp) \delta^2(k'_\perp - k_\perp) \\ &= \int d^2 x_\perp e^{-ix_\perp(k'_\perp + p'_\perp)} \tilde{W}_{x_\perp}^A(k'_\perp - k_\perp). \end{aligned} \quad (38)$$

This provides us with the final result of the total amplitude,

$$\mathcal{T}_{ij} = \frac{-i\lambda q_+}{2(2\pi)^2} \int d^2 k_\perp \frac{N^2 \delta_{ij} + 2k_i k_j}{N^2 + k_\perp^2} \int d^2 x_\perp e^{-ix_\perp(k'_\perp + p'_\perp)} \tilde{W}_{x_\perp}^A(k'_\perp - k_\perp). \quad (39)$$

The cross section in Eq. (12) is obtained by means of the standard formula for scattering off an external field,

$$\sigma_{sc}^{(1)}(x, Q^2) = \frac{1}{2} \int \frac{d^3 k'}{(2\pi)^3 2k'_0} \frac{d^3 p'}{(2\pi)^3 2p'_0} \frac{1}{2q_0} 2\pi \delta(k'_0 + p'_0 - q_0) |\mathcal{T}_{ij}|^2, \quad (40)$$

where the two identical particles in the final state require the factor 1/2 in front of the integral.

C Evaluation of the integral with the function W^A

In this appendix we present some details of the derivation of Eq. (22). To introduce the integration variable z we exploit the relation $k'^2_\perp / (\alpha(1-\alpha)) = M^2 = Q^2(1-z)/z$. Therefore the k'_\perp integration appearing on the l.h. side of Eq. (22) can be replaced according to

$$\int \frac{dk'^2_\perp}{\alpha(1-\alpha)} \longrightarrow Q^2 \int^1 \frac{dz}{z^2}, \quad (41)$$

where just the leading contribution at small z is kept. Concerning the lower bound of the z integration we refer to the discussion given in Sect. 5.

Subsequently, it is convenient to divide the α integration of Eq. (22) in two parts by introducing an arbitrary parameter μ' which fulfills the condition $\Lambda^2 \ll \mu'^2 \lesssim Q^2$. To be specific we separate the symmetric and asymmetric gluon configurations in the integration by means of

$$\int d\alpha = \int_{\mu'^2/M^2}^{1-\mu'^2/M^2} d\alpha + 2 \int_0^{\mu'^2/M^2} d\alpha, \quad (42)$$

where the symmetric (asymmetric) configurations give rise to the first (second) term on the r.h. side of Eq. (22). For a given value of M^2 the symmetric contribution contains large transverse momenta k'_\perp while the asymmetric term is entirely soft.

To extract the leading twist of the symmetric hard part we use

$$\int d^2 k_\perp \frac{N^2 \delta_{ij} + 2k_i k_j}{N^2 + k_\perp^2} \tilde{W}_{x_\perp}^A(k'_\perp - k_\perp) = C_{ij,a} \int d^2 k_\perp k_a \tilde{W}_{x_\perp}^A(-k_\perp) + \text{higher twist}, \quad (43)$$

$$\text{with } C_{ij,a} = 2 \left(\frac{k'_i \delta_{ja} + k'_j \delta_{ia}}{N^2 + k_\perp'^2} - \frac{k'_a (N^2 \delta_{ij} + 2k'_i k'_j)}{(N^2 + k_\perp'^2)^2} \right).$$

The simple relations

$$C_{ij,a} C_{ij,b} = \frac{4z(1-z)(1+z^2)}{N^2} \delta_{ab}, \quad \text{and} \quad (44)$$

$$\left| \int d^2 k_\perp k_a \tilde{W}_{x_\perp}^A(-k_\perp) \right|^2 = (2\pi)^4 \left| \partial_\perp W_{x_\perp}^A(0_\perp) \right|^2 \quad (45)$$

are important for the further evaluation of the hard contribution. In writing Eq. (44) we have anticipated the symmetric k'_\perp integration and employed the substitution $k'_a k'_b \rightarrow k_\perp'^2 \delta_{ab}/2$. Finally, performing the α integration and keeping only the contribution that is dominant at small z , the first term on the r.h. side of Eq. (22) is obtained.

In the case of the asymmetric soft contribution, which is independent of Q^2 and therefore leading twist, the α integration is replaced by an integral over k'_\perp . Since α is small we have $Q^2 \alpha \simeq k_\perp'^2 z$, leading to the replacement

$$\int_0^{\mu'^2/M^2} d\alpha \simeq \frac{z}{Q^2} \int_0^{\mu'^2} dk_\perp'^2. \quad (46)$$

The remaining step to obtain the second term on the r.h. side in Eq. (22) is the k_\perp integration. Keeping in mind that for the soft term we can neglect N^2 this integration can easily be done with the aid of

$$\int dk_\perp^2 \frac{k_i k_j}{k_\perp^2} e^{ik_\perp y_\perp} = \frac{2\pi}{y_\perp^2} \left(\delta_{ij} - \frac{2y_i y_j}{y_\perp^2} \right). \quad (47)$$

D Simplification of the final expression

In this appendix, the details of the derivation of Eq. (29), which represents a particularly simple form of our final result, are described.

It is convenient to introduce a real parameter $\epsilon > 0$ and to write the gluon distribution given by Eqs. (23) and (27) in the form

$$xg^{(1)}(x, \mu^2) = \frac{2}{\pi^2} \left(\ln \frac{1}{x} \right) I_0(0, \mu'), \quad (48)$$

where

$$I_\epsilon(a, b) \equiv \int_{a^2 < k_\perp'^2 < b^2} d^2 k'_\perp f_\epsilon(k_\perp'^2), \quad (49)$$

$$f_\epsilon(k'_\perp{}^2) \equiv \int \frac{d^2 y_\perp}{(2\pi)^2 y_\perp^{2-\epsilon}} \int \frac{d^2 z_\perp}{(2\pi)^2 z_\perp^{2-\epsilon}} h(y_\perp, z_\perp) e^{ik'_\perp(y_\perp - z_\perp)} \left(\frac{2(y_\perp z_\perp)^2}{y_\perp^2 z_\perp^2} - 1 \right), \quad (50)$$

and

$$h(y_\perp, z_\perp) \equiv \int d^2 x_\perp \text{tr} \left[W_{x_\perp}^A(y_\perp) W_{x_\perp}^{A\dagger}(z_\perp) \right]. \quad (51)$$

Furthermore, we have

$$I_0(0, \mu') = \lim_{\epsilon \rightarrow 0} [I_\epsilon(0, \infty) - I_\epsilon(\mu', \infty)]. \quad (52)$$

The k'_\perp integration in the definition of $I_\epsilon(0, \infty)$ is easily performed giving a δ -function of $y_\perp - z_\perp$. The result is

$$I_\epsilon(0, \infty) = \int \frac{d^2 y_\perp}{(2\pi)^2 y_\perp^{4-2\epsilon}} h(y_\perp, y_\perp). \quad (53)$$

Since

$$h(y_\perp, z_\perp) \simeq C y_\perp \cdot z_\perp \quad \text{for} \quad |y_\perp|, |z_\perp| \ll 1/\Lambda, \quad (54)$$

where C is a constant, one can write

$$I_\epsilon(0, \infty) = \frac{C}{2\pi} \frac{r^{2\epsilon}}{2\epsilon} + \frac{1}{4\pi} \int_{r^2 < y_\perp^2} \frac{dy_\perp^2}{y_\perp^4} h(y_\perp, y_\perp) + \mathcal{O}(\epsilon). \quad (55)$$

The parameter r has been introduced to separate the small-distance from the large-distance part of the y_\perp integration.

In the k'_\perp integration defining $I_\epsilon(\mu', \infty)$, the momentum variable k'_\perp is always large. Therefore, the result is only sensitive to the small distance structure of $h(y_\perp, z_\perp)$, and we can write

$$I_\epsilon(\mu', \infty) = \int_{\mu'^2 < k'_\perp{}^2} d^2 k'_\perp \int \frac{d^2 y_\perp}{(2\pi)^2 y_\perp^{2-\epsilon}} \int \frac{d^2 z_\perp}{(2\pi)^2 z_\perp^{2-\epsilon}} C y_\perp \cdot z_\perp e^{ik'_\perp(y_\perp - z_\perp)} \left(\frac{2(y_\perp z_\perp)^2}{y_\perp^2 z_\perp^2} - 1 \right). \quad (56)$$

This integral can be calculated using standard methods:

$$I_\epsilon(\mu', \infty) = \frac{C}{2\pi^2} \frac{\mu'^{-2\epsilon}}{2\epsilon} \left[\left(\frac{\Gamma(1+\epsilon)\Gamma(\frac{1-\epsilon}{2})}{\Gamma(1-\frac{\epsilon}{2})} \right)^2 (1+\epsilon) + \mathcal{O}(\epsilon^2) \right]. \quad (57)$$

When inserting Eqs. (55) and (57) in Eq. (52), the poles in ϵ cancel. Setting the parameter r , which so far was arbitrary, to

$$r(\mu)^2 = \frac{4e^{1-2\gamma_E}}{\mu'^2} = \frac{4e^{\frac{1}{12}-2\gamma_E}}{\mu^2}, \quad (58)$$

the result of Eq. (29) follows. Here γ_E is Euler's constant.

References

- [1] V.N. Gribov and L.N. Lipatov, Sov. J. Nucl. Phys. 15 (1972) 438, 675;
G. Altarelli and G. Parisi, Nucl. Phys. B126 (1977) 298;
Yu.L. Dokshitzer, Sov. Phys. JETP 46 (1977) 641
- [2] E.A. Kuraev, L.N. Lipatov and V.S. Fadin, Sov. Phys. JETP 44 (1976) 443 and 45 (1977) 199;
Y.Y. Balitsky and L.N. Lipatov, Sov. J. Nucl. Phys. 28 (1978) 822;
J. Bartels, Nucl. Phys. B151 (1979) 293 and B175 (1980) 365;
A.H. Mueller, Nucl. Phys. B415 (1994) 373;
N.N. Nikolaev and B.G. Zakharov, Z. Phys. C64 (1994) 631
- [3] A. Donnachie and P.V. Landshoff, Nucl. Phys. B244 (1984) 322, Phys. Lett. B296 (1992) 227 and B437 (1998) 408;
J.R. Cudell, A. Donnachie and P.V. Landshoff, Phys. Lett. B448 (1999) 281;
K. Golec-Biernat and M. Wüsthoff, Phys. Rev. D59 (1999) 014017;
U. D'Alesio, A. Metz and H.J. Pirner, Eur. Phys. J. C9 (1999) 601
- [4] O. Nachtmann, Ann. Phys. 209 (1991) 436
- [5] H.G. Dosch and A. Krämer, Phys. Lett. B252 (1990) 669
- [6] H.G. Dosch, T. Gousset and H.J. Pirner, Phys. Rev. D57 (1998) 1666
- [7] I. Balitsky, Phys. Rev. D60 (1999) 014020;
J. Jalilian-Marian, A. Kovner and H. Weigert, Phys. Rev. D59 (1999) 014015
- [8] W. Buchmüller, M.F. McDermott and A. Hebecker, Nucl. Phys. B487 (1997) 283;
B500 (1997) 621 (E)
- [9] W. Buchmüller, T. Gehrmann and A. Hebecker, Nucl. Phys. B537 (1999) 477
- [10] H.G. Dosch, Phys. Lett. B190 (1987) 177;
H.G. Dosch and Yu.A. Simonov, Phys. Lett. B205 (1988) 339
- [11] F. Hautmann, Z. Kunszt and D.E. Soper, Phys. Rev. Lett. 81 (1998) 3333;
Yu.V. Kovchegov and L. McLerran, Phys. Rev. D60 (1999) 054025
- [12] A.H. Mueller, Nucl. Phys. B335 (1990) 115
- [13] A.H. Mueller, preprint CU-TP-937 (hep-ph/9904404)
- [14] W. Buchmüller, talk at *New Trends in HERA Physics*, Ringberg Workshop 1999 (hep-ph/9906546)
- [15] L. McLerran and R. Venugopalan, Phys. Rev. D49 (1994) 2233
- [16] Yu.V. Kovchegov, Phys. Rev. D54 (1996) 5463 and D55 (1997) 5445;
Yu.V. Kovchegov and A.H. Mueller, Nucl. Phys. B529 (1998) 451

- [17] A. Hebecker and H. Weigert, Phys. Lett. B432 (1998) 215
- [18] S.J. Brodsky and P. Hoyer, Phys. Lett. B298 (1993) 165
- [19] A. Hebecker, preprint HD-THEP-99-12 (hep-ph/9905226)